Superconducting Reluctance and Hysteresis Electrical Motors

A. Leão Rodrigues

Department of Electrical Engineering
Faculty of Science and Technology
New University of Lisbon
2829 - 516 Caparica **PORTUGAL**
Fax: +351 21294 8532 E-mail: leao@uninova.pt

Abstract

The paper is devoted to the Electrical Machines on the basis of new materials for electro mechanics high temperature superconductors [1]. At present, high temperature superconductors (HTS) are already widely used in power applications. This allows improving essentially the output power and size of the electrical machines. In the wide variety of HTS power devices the essential relates on electrical machines. The progress in HTS materials gives a strong impulse for elaborating new layouts of HTS machines [2].
Theoretical and experimental researches show that the HTS electrical machines possess higher values of specific output power, efficiency and power factor compared with conventional electrical machines [3]. Some experimental results obtained from a conventional 2 kW stator with different superconductors rotors are displayed in the paper.
It is expected that HTS electrical machines will find a wide range of application in different areas of modern engineering such as on-land power stations and aerospace.

1. - INTRODUCTION

It is expected that electrical machines having superconducting components will have a high power density, allowing conventional machines to be replaced by smaller superconducting ones. The disadvantage is the need to cool the superconductors and the increased performance must justify this extra effort. Possible pplications include the pumping of cryogen in space where, provided there is adequate solar shielding the temperature is already appropriate.
The great disadvantage of the HTS materials in the construction of power devices is its brittle nature and thus the difficulty to be machined. When using HTS materials in electric machines much care must be taken in the design of the rotors in order to eliminate mechanical stresses in these fragile materials. Perhaps, reluctance and hysteresis rotors are the best candidates to employ these materials in their construction and different configurations, giving different torques, are now considered.
Due to the unique way in which superconductors respond to the magnetic fields, it is difficult to predict how a machine will perform. The state of art of four different types of HTS electric machines is presented in the paper.

2. – MEISSNER MOTOR

The Meissner motor is a good example to illustrate the diamagnetic behaviour of the superconductor materials. When a superconductor is placed in a magnetic field it behaves as a flux shield due to the persistent electric currents induced at its surface. In consequence the superconductor experiments a repulsion force from the magnetic field, as shown in figure 1. This phenomenon was discovered in 1932 by Meissner e Ochsenfeld.

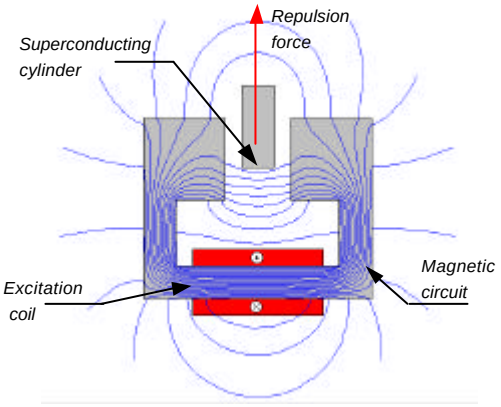

Fig. 1 – Meissner effect

After the discovery of HTS materials in 1986, a prototype of the Meissner Motor was constructed in Japan. The rotor consists of a certain number of cylinders of YBCO superconducting material that passes through the air gap of a excited electromagnet bathed by liquid nitrogen, as shown in figure 2. The HTS cylinders outside the liquid nitrogen are in normal state and so can easily penetrate inside the air gap. In this region, however, they attain the superconductor state and therefore a repulsion force due to the magnetic field is experimented, generating a torque on the shaft and producing a continuous rotor rotation.

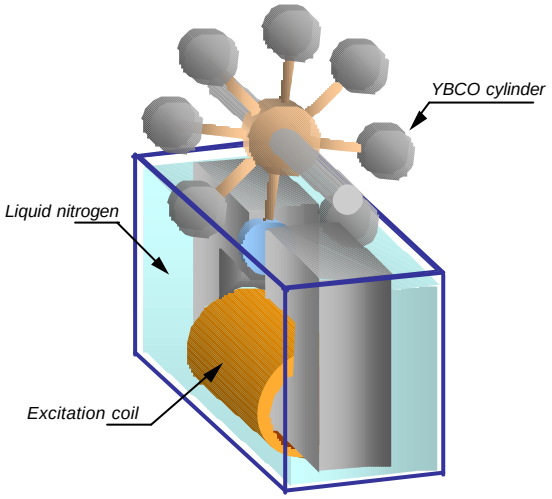

Fig. 2 – Meissner motor

The rotor speed ω of this motor is rather low but the torque T is relatively high, giving a moderate output power $P=T\omega$. This kind of motor illustrates a very unusual approach to the directed energy conversion of the heat energy into the mechanical power one on the base of HTS materials.

3. – SALIENT TYPE HTS RELUCTANCE MOTOR

The flux plot of a conventional two pole reluctance motor is shown in figure 3a, where some leakage flux takes place. A low reluctance along the rotor direct axis gives high inductance L_{max} and a high reluctance along the quadrature axis gives a low inductance L_{min} to the stator winding. Assuming sinusoidal variation, figure 3b shows plotted the inductance stator winding variation $L(\theta)$ according to rotor position θ.

The torque produced in a three-phase reluctance motor is given [4] by

$$T(\theta) = \frac{3}{2} I^2 \frac{dL(\theta)}{d\theta} = -\frac{3}{2} I^2 (L_{max} - L_{min}) sen2\theta \qquad (1)$$

as shown plotted in figure 3c.

Eq.(1) shows that in order to increase maximum torque the inductance difference (L_{max} -L_{min}) must be improved.

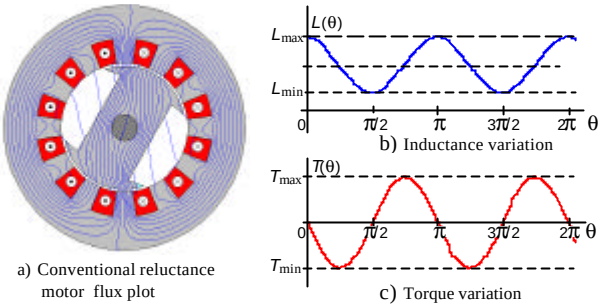

Fig.3 – Conventional reluctance motor and torque variation

This can be achieved by eliminating rotor leakage flux. Attaching two blocks of HTS flanking the rotor, the difference (L_{max} -L_{min}) is improved since induced currents in the HTS components will prevent flux transverse the quadrature axis and tend to encourage flux along the direct axis. In this scheme shown in figure 4a, HTS blocks work as the concentrators of the magnetic flux along the direct axis.

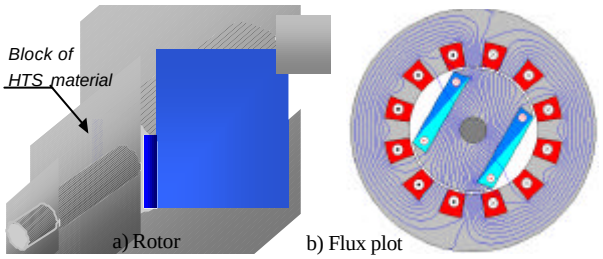

Fig.4 – HTS reluctance motor layout and flux plot

The HTS pieces are electrically separated so that all super current loops must originate and return in the same piece and currents can not transverse the iron. Figure 4b illustrates the flux plot for this new construction where the leakage flux almost disappears. Although this construction is a bit complicated the mo tor has good starting characteristics [5].

4. – "ZEBRA" TYPE HTS RELUCTANCE MOTOR

Another possible configuration is the composite or "zebra" type rotor. Slices of iron and superconducting ceramics are assembled as shown in figure 5a. Slices

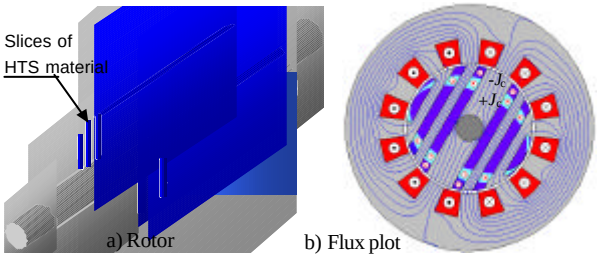

Fig.5 – HTS "Zebra" reluctance motor layout and flux plot

of YBCO or Bi-Ag elements can be used and a strong and balanced rotor is obtained. Again, the flux has an easy path along the longitudinal axis and a great reluctance along the transversal axis that results also in a considerable difference between the maximum and minimum inductance and consequently a high torque is produced. Figure 5b shows the flux plot produced by the stator winding in the composite rotor. It can be seen that, as in the case of salient type, transport currents $+J_c$ and $-J_c$ are circulating axially in each block, which penetrate about half of the ratio of the rotor [5].
The optimal torque is obtained when the iron and HTS plates have both the same thickness. However, due to the installation of the shaft the middle iron block is thicker.

5. – NOVEL SYNCHRONOUS MACHINE

The longitudinal ends of the two HTS blocks of the reluctance motor can be electrically connected, forming a coil of one single turn, as shown in figure 6a. This allows the pre-magnetisation of the rotor and the machine behaves as a permanent magnet synchronous one [6]. The magnetic flux set up by the pre-magnetised HTS rotor and by stator on load is illustrated in figure 6b.

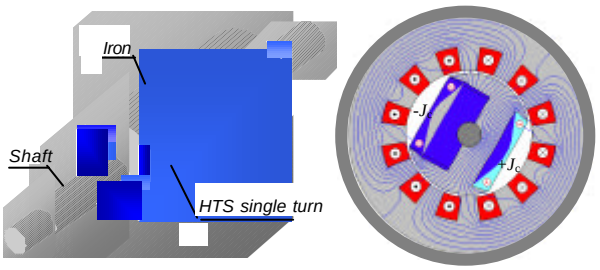

Fig.6 – HTS rotor of a synchronous machine and flux plot

In this case super currents can circulate the iron rotor and forming surrounding loops $+J_c$ and $-J_c$, like a field winding and the rotor behaves as the best-known permanent magnet for the same equivalent volume of the superconductor.
The output torque has now the reluctance component $T_R = A\sin 2\theta$ and an synchronous torque component $T_E = B\sin\theta$, giving a high resulting torque

$$T = A\sin 2\theta + B\sin\theta\,. \qquad (2)$$

Because the synchronous or excitation torque is usual much greater than reluctance torque, the resulting torque variation has now one cycle per rotor revolution, as shown in figure 7.
The stator winding can be used to pre-magnetise the superconductor by field cooling. It is important that the pre-magnetising field penetrates further than the rotating field, otherwise, during the normal operation the trapped field can be lost.

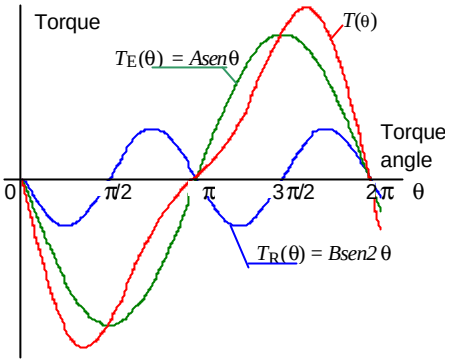

Fig.7 - Torque variation of a salient pole synchronous motor

The sequence of the HTS coil pre-magnetisation is illustrated in figure 8. With the ceramic material in the normal state, $T > T_c$, a static stator field is switched on. A flux density of about twice of the flux during normal operation is desirable. The second step is to cool the HTS rotor with liquid nitrogen at temperature $T < T_c$ and maintaining the stator field. The HTS material attains the superconducting state by field cooling.

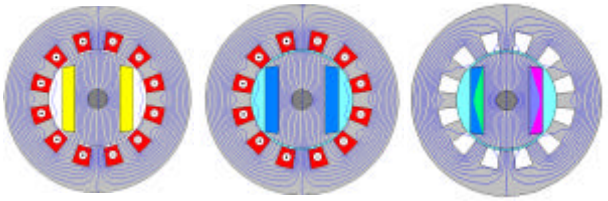

a) Stator switched on $T>T_c$ b) Stator switched on $T<T_c$ c) Stator switched off $T<T_c$

Fig.8 – Sequence of the HTS coil pre-magnetisation

Finally, the stator current is switched off and super currents are induced in the superconductor penetrating further in the material. Therefore the rotor retains some trapped flux behaving as a permanent magnet. The situation is maintained while the HTS material of the rotor is kept with a temperature $T < T_c$.
Figure 9 shows a cross section of a HTS synchronous machine, including the cryostat system, with a rated

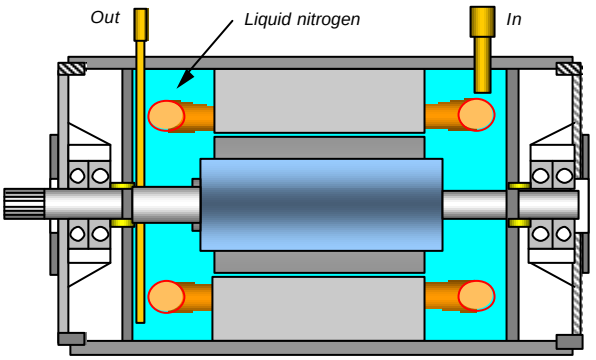

Fig.9 – Cryostat system of the HTS synchronous machine

output power of 780 kW, 12000 rpm and 400 Hz. The volume aspect ratio of this machine compared with a conventional one of the some characteristics is about six times less, giving to this design a near future application in aerospace industry.

6. – THEORETICAL TORQUE COMPARISON

Figure 10 shows a comparison of the salient, composite and pre magnetised synchronous torques by the previous machines, relative to the conventional reluctance torque. The theoretical results show that the torque produced by the HTS *salient type motor* is about 1.7 times greater than the torque produced by the conventional motor and the HTS *composite type*, with five iron blocks and six YBCO blocks on the rotor, is about 2.2 times greater, but the construction is more complicated and expensive than that of salient pole.

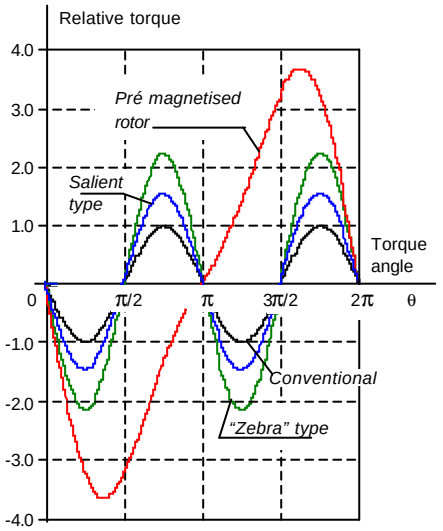

Fig.10 – Relative developed torque comparison

However, the total torque givem by Eq.(1) developed in the *pre-magnetised rotor* is 3.7 times greater than the correspondent conventional reluctance torque.

7. - EXPERIMENTAL RESULTS

The previous four rotors were tested using the same conventional two pole three-phase 2 kW stator. Each motor was cooled in a liquid nitrogen container. A powder break was used to measure the output torque and the test rig is shown in figure 11. When the HTS material of the rotor attained the critical temperature, the stator was switched on to 230/400 V, 50 Hz source.
Due to a small rotor cage, the motor has asynchronous/ synchronous self starting characteristics.

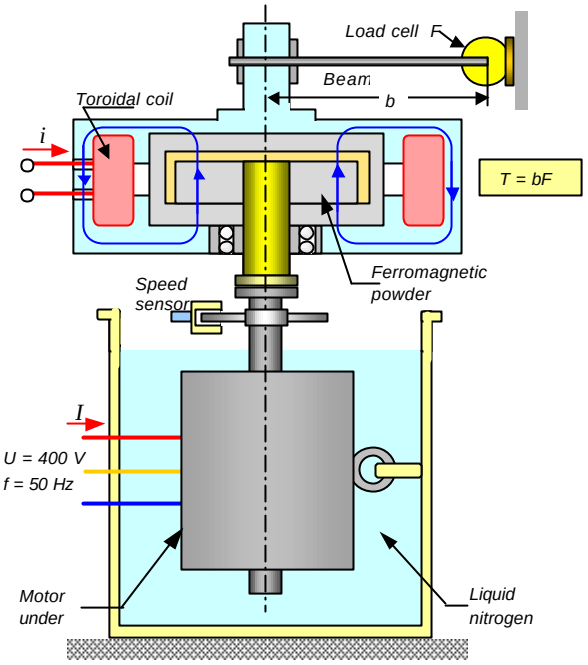

Fig. 11 – Powder break test rig for torque measurement

By varying the excitation current *i* of the toroidal coil, friction of the ferromagnetic powder generates output motor torque. Force in the end of a beam of length b is measured by means a load cell giving the mechanical torque $T = bF$. Figure 12 shows experimental results of

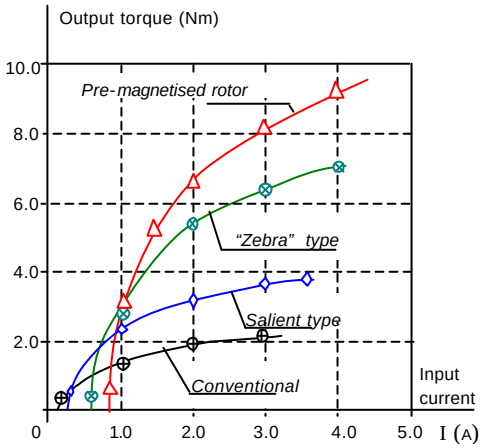

Fig.12 - Output torque versus stator current.

torque versus input current for each type of rotor. For the reluctance motor the "Zebra type" presents the best torque. However its construction is a bit more sophisticated. Pre magnetised synchronous motor presents obviously the higher torque. These results agree with the experimental results obtained by Kovalev [7].

8. - HTS HYSTERESIS MOTOR

When a cylinder of HTS material is placed in a variable magnetic field, superficial currents are induced on the material originating hysteresis losses. The persistent currents on the rotor generate a magnetic flux that reacting with the stator flux produces a electromechanical torque. It can be shown [8] that this torque is proportional to the rotor hysteresis losses, and this is the reason why the device is called hysteresis motor. It is also shown that, contrary to conventional electric motors (e.g. synchronous, asynchronous, hysteresis), the torque of the HTS hysteresis motor results from repulsion of the magnetic poles induced into HTS rotor by the rotating field of the stator winding.

Figure 13a shows the flux distribution in a type-II superconductor cylinder of low critical current density J_c placed in a rotating field and figure 13b a similar cylinder of higher critical current density J_c. Comparison of both plots shows that as the critical current density increases more flux crosses the periphery of the cylinder, leaving the interior inactive.

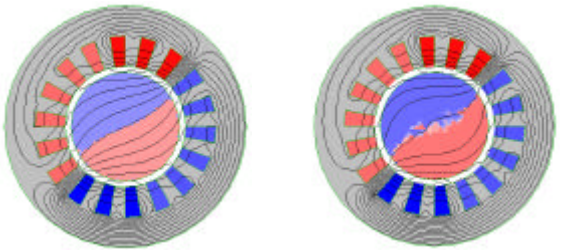

a) Low critical current density b) High critical current density

Fig.13. Flux penetration in a type-II HTS cylinder

For a HTS cylinder of volume $Vol = (\pi/4)D_o^2\ell$ of diameter D_o and effective length ℓ, placed in a rotating field with an air gap sinusoidal distribution of amplitude $\hat{B}$ reference [5] gives the following torque expression

$$T = \frac{1}{3\pi}\ell D_o^3 J_c \hat{B}\beta(\delta) \quad \text{where} \quad \beta(\delta) = 1 - \frac{1}{\alpha\delta^{2.2}+1}$$

is a dimensionless factor which characterizes the flux penetration. The parameters α and $\delta = (4/\pi)\hat{B}/\mu_o J_c D_o$ depend on the HTS material properties and rotor diameter D_o. For a $2p$ pole hysteresis motor the torque per prismatic rotor volume $D_o^2\ell$ reduces to

$$T_u = \frac{T}{D_o^2\ell} = \frac{p}{3\pi} D_o J_c \hat{B}\beta(\delta) \qquad (3)$$

and increases with rotor diameter.

For HTS materials with small flux penetration, i.e, high J_c, torque can be increased using a ring with a inner diameter D_i. For rotors with this geometry specific torque expression reduces to

$$T_u = \frac{p}{3\pi} D_o J_c \hat{B}\left[1 - \left(\frac{D_i}{D_o}\right)^3\right]\beta(\delta) \qquad (4)$$

Eq.(4) shows that , as it happens in a conventional hysteresis motor, torque is independent of rotor speed. Computing simulations show that the optimal torque is obtained when $D_i = 0{,}78D_o$, i.e., when the HTS ring width is about 11% of outer rotor diameter. Increasing od D_i generates decreasing of torque, which is obviously zero when $D_i = D_o$.

The configuration of HTS hysteresis machine is shown in figure 14a. The rotor consists of HTS cylindrical elements. Each element can be manufactured as whole cylinder or can be glued from circular sectors in such way that the HTS C axis has the radial orientation.

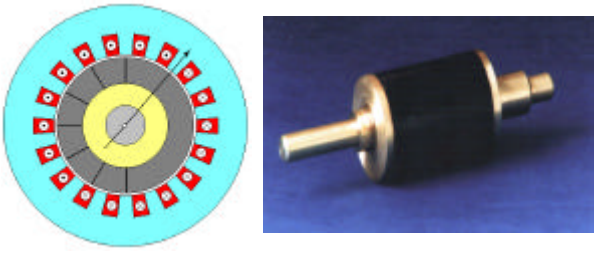

a) Hysteresis motor layout b) HTS rotor aspect

Fig. 14 – Hysteresis motor topology

In spite of the HTS material brittleness the rotor constructed in this way is very robust. Figure 14b shows a photograph of a hysteresis rotor constructed with several circular sectors.

Figure 15a shows the flux plot for a rotor using four sectors and figure 15b for a rotor using six circular sectors. The plots show that the flux penetration inside the rotor increases with increasing the number of HTS circular sectors. due to the epoxy resin between them. Therefore, torque developed will decrease with the number of sectors. Although circular sectors are easier to be produced the number used in the rotor construction should be limited.

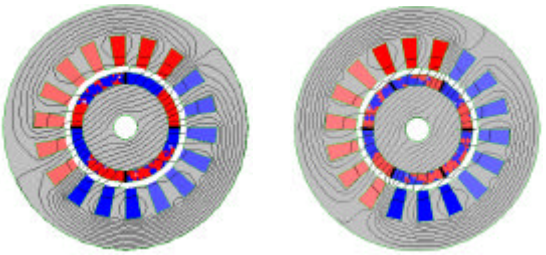

a) Rotor with four sectors b) Rotor with six sectors

Fig. 15 – Flux plot for rotors employing different circular sectors

A hysteresis motor with a single ring of YBaCu rotor with a critical current density of $J_c = 3{,}5x10^7$ A/m^2 was tested. For comparison, a conventional hysteresis motor with a large ferromagnetic hysteresis loop was also tested. In figure 16 are displayed, in the same scale, results of torque per prismatic rotor volume versus stator current density J_s for both type of motors.

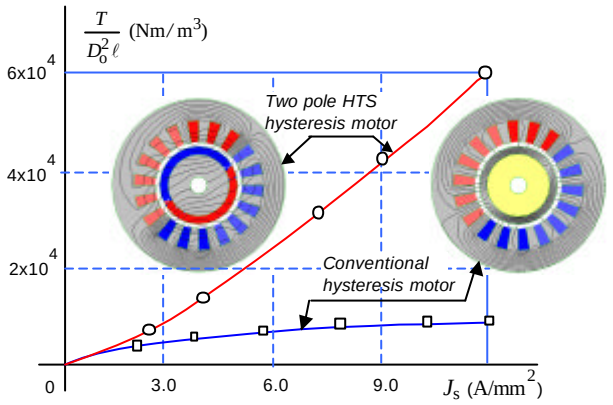

Fig. 16 – Specific torque versus stator current density for conventional and HTS hysteresis motors

Specific torque of HTS hysteresis motor increases almost with the stator current density squared, while for the conventional hysteresis motor is almost constant. The ratio of torque is however of the order of six times.

9. - CONCLUSIONS

HTS materials are able to change considerably the future power systems in this century because they give the new active materials having unique properties. Compared with conventional motors HTS motors have specific torque of the order of six times, which makes these devices very powerful machines. However, in order to obtain these performances the rotor must be cooled under the critical temperature of the superconductor. Nevertheless, in locals where installations of liquid nitrogen or liquid hydrogen are available, such as in the near future hydrogen-powered aircrafts (cryoplanes) and other land vehicles, where volume and weight are undesirable, these type of machines can be serious competitors of conventional motors.

ACKNOWLEDGEMENT

This work was supported by the RTN Supermachines Project nº HPRN-CT-2000-00036. Thanks are also due to Prof. David Dew-Hughes from Department Engineering Science, University of Oxford, and Prof. Leo Kovalev from Moscow Aviation Institute for the stimulating discussions about HTS motors.

REFERENCES

[1] Bednorz J.G., and Müller K.A., *Possible High T_c Superconductivity in the Ba-La-Cu-O System*", Z. Phys. B, 64 1986.

[2] McCulloch, M. and Dew-Hughes,D: *Brushless ac machines with high temperature superconduc-ting rotors*, Material Science and Engineering B, Elsivier, 1998.

[3] Depart. Engineering Science University of Oxford, U.K.; Moscow State Aviation Institute, Moscow, Russia; Institut fuer Physikalische Hochtechnologie, Jena, Germany, Institute de Ciencia de Materials de Barcelona, Bellaterra, Spain; DEE-FCT/UNL, Caparica, Portugal.

[4] Barnes G J, McCulloch M, Dew-Hughes: *Applications and modelling of bulk HTS in brushless AC machines, Supercond*. Sci.Technology, 13 875-878, 2000.

[5] Barnes G. J.: *Computational modelling for type-II superconductivity and the investigation of high temperature superconducting electrical machines*, Ph.D. Thesis, Oxford University, 2000.

[6] Barnes G. J., Dew-Hughes D., McCulloch M., Torque from hysteresis machines with type-II superconducting segmented rotors, *Physica C*, 331(2000), 133-140.

[7] Kovalev L.K. et al., HTS motors design. Recent results and future development, *Superconductivity Research and Development, 1996.*

[8] Kovalev L.K. et al., Hysteresis and reluctance electric machines with bulk HTS rotor elements, *IEEE Trans. on Applied Superconductivity*, 9(1999), 1261.

* * *